A Network Study of Gene Expression Across Human Brain Development

Guillem Chillon[a,b,1]

This manuscript was compiled on December 3, 2025

The human brain undergoes extensive functional and structural reorganization from the fetal period through adulthood, characterized by a shift from local, anatomically driven connectivity to distributed, functionally specialized networks. However, the transcriptomic architecture underlying this macro-scale reorganization remains poorly understood. Using the BrainSpan developmental transcriptome atlas, I constructed stage-specific gene co-expression networks for cortical and subcortical functional brain systems across four developmental age stages (Fetal, Infant, Adolescence, and Adult). I used network neuroscience to measure topological integration and segregation, and network control theory to model the energy transitions of these transcriptomic networks. Comparing the two functional systems reveals a fundamental divergence in developmental timing and topology. While both the cortical and the subcortical systems begin with the same trajectory in the Prenatal period, their maturation paths diverge postnatally. The Prefrontal Cortex follows a U-shaped trajectory for modularity and an inverse U-shape for efficiency, prioritizing integration in infancy before stabilizing into specialization. In contrast, the Limbic System follows an N-shaped trajectory, characterized by a unique period of topological isolation (hyper-segregation and reduced efficiency) during adolescence. These findings suggest that the molecular wiring of the brain undergoes a system-specific reorganization, providing a framework for understanding the timing of neurodevelopmental vulnerability.

Gene co-expression networks | Network neuroscience | Neurodevelopmental biology

Significance Statement

Human brain development involves a profound reorganization from a flexible, rapidly growing fetal system to a specialized, cognitively advanced adult system. While this shift is well-documented in functional MRI studies, the underlying molecular architecture driving these changes remains unknown. This study reveals that the transcriptomic architecture of the brain does not mature uniformly but follows system-specific topological trajectories. While the prefrontal cortex prioritizes global integration during infancy to support rapid learning, the limbic system undergoes a unique period of topological isolation during adolescence.

The human brain is not a static organ; it undergoes a structural and functional metamorphosis from the fetal period through adulthood (1). Neuroimaging studies using functional MRI (fMRI) have established that this maturation follows a specific trajectory: infants exhibit "local" connectivity driven by anatomical proximity, while adults develop "distributed" networks driven by functional specialization (2–4). This reorganization involves a hub shift, where the control centers of the brain move from primary sensory and motor regions in infancy to higher-order association cortices, such as the default mode and frontoparietal networks in adulthood (3).

While the topological reorganization of the brain is well-characterized at the macro-scale, the micro-scale molecular architecture driving this process remains elusive. Gene expression provides the fundamental blueprint for brain structure, but most transcriptomic studies focus on differential expression of individual genes rather than the architecture of the gene regulatory networks themselves(5–8). Previous work has begun to bridge this gap; notably, Richiardi et al. (2015) demonstrated that correlated gene expression patterns in the adult brain significantly overlap with functional connectivity networks measured by fMRI, linking synaptic gene expression to synchronous brain activity (9). However, this study was restricted to a static adult timepoint, leaving a gap in our understanding: does the transcriptomic activity of the brain evolve dynamically across the lifespan as functional brain networks (fMRI) does? Determining if the micro-scale (transcriptome) mirrors the macro-scale (fMRI) trajectory will help understand whether functional neurodevelopment is a direct consequence of coordinated gene expression or if other additional variables drive these changes.

Using the BrainSpan developmental transcriptome atlas (10), I constructed gene co-expression networks across development for two different functional brain systems: Prefrontal Cortex (neocotical system) and Limbic System (sub-cortical dominated system). Comparing these systems allowed me to determine if cortical and subcortical networks mature distinctly. I first characterized the structural reorganization of these networks quantifying network efficiency and modularity to track the developmental shifts between integration and segregation. Complementing this topological view, I applied Network Control Theory (NCT) by treating

Author affiliations: [a]Bioengineering Graduate Program, School of Engineering and Applied Science, University of Pennsylvania, Philadelphia, PA, USA; [b]Raymond G. Perelman Center for Cellular and Molecular Therapeutics, The Children's Hospital of Philadelphia, Philadelphia, PA, USA

Author performed all data analysis, interpreted results, and wrote the manuscript.

The authors declare no competing interests.

[1]To whom correspondence should be addressed. E-mail: guillemc@upenn.edu

gene expression levels as energy inputs. This allowed me to quantify the brain's capacity for average controllability (the ability to move into easy, nearby states, representing plasticity) versus modal controllability (the ability to move into difficult, distant states, representing specialization) (11, 12). My results reveal that cortical and subcortical circuits follow divergent topological trajectories, with the Prefrontal Cortex prioritizing plasticity and integration during infancy, while the Limbic system undergoes a distinct period of network isolation during adolescence.

Results

Transcriptome Reorganizes Across Development. To characterize macro-scale reorganization of the human brain transcriptome, I first examined global gene expression patterns across the lifespan. I analyzed RNA-sequencing data from the BrainSpan atlas (10), encompassing 162 samples from 32 different donors spanning from 8 post conception weeks (pcw) to 40 years of age. Donors were grouped into four developmental stages based on established structural milestones (13): Prenatal (8 - 37 pcw), Infancy (4 months - 4 years), Youth/Adolescence (8 - 21 years), Adulthood (23+ years).

Hierarchical clustering of all samples revealed a temporal gradient, with prenatal samples forming a distinct, tightly correlated cluster separated from postnatal life (Figure 1A). This suggests that the largest transcriptomic reconfiguration occurs at birth. Principal component Analysis (PCA) of all samples confirmed this trajectory (Figure 1B), showing a developmental progression where the prenatal state is transcriptomically distant from all others. On the other hand, infancy is situated between the fetal samples and the mature brain, while adolescence and adult samples cluster together.

Architectural Shift in Functional Connectivity in the Prefrontal Cortex. To study the specific wiring changes underlying these global shifts, I constructed gene co-expression networks for two different functional systems - the frontal cortex (dorsolateral prefrontal cortex [DFC], ventrolateral prefrontal cortex [VFC], anterior (rostral) cingulate (medial prefrontal) cortex [MFC]) and limibic system (amygdaloid complex [AMY], hippocampus [HIP], orbital frontal cortex [OFC]) - using the top 300 most variable genes per each system (Figure 2. In these networks, nodes represent individual genes, and edges represent the strength of co-expression between gene pairs across the brain functional system.

I next quantified the topological reorganization of each system by calculating graph theory metrics for each individual donor.

For the Prefrontal Cortex (Figure 3), global efficiency, a measure of network integration, exhibited a significant developmental trajectory (ANOVA $p < 0.001$). Efficiency peaked during Infancy (0.657, $p_{adj} =< 0.001$ when compared to prenatal) before decreasing to Adulthood (0.618) to levels statistically indistinguishable from the prenatal baseline ($p_{adj} = 0.27$). This suggests that during infancy, the prefrontal cortex prioritizes rapid integration of information, a feature that it is reduced as the brain matures. Concurrently, modularity followed a U-shaped trajectory ($p < 0.001$), dipping to its lowest point in infancy ($p_{adj} = 0.002$ vs prenatal) before increasing again in Adulthood ($p_{adj} = 0.87$ vs prenatal). This indicates that the gene network undergoes a transient period of high inter-connectivity in early postnatal phases, before re-establishing a segregated community structure in adulthood.

By applying Network Control Theory (NCT) to model the energy landscape, I found significant shifts in control properties. Average controllability was significantly elevated in the infant and adolescence stages compared to prenatal ($p_{adj} < 0.001$), with infancy also showing significantly higher plasticity than adolescence ($p_{adj} = 0.015$) and adulthood ($p_{adj} = 0.004$). Additionally, modal controllability showed a similar inverted U shape trajectory as average controllability.

Architectural Shift in Functional Connectivity in the Limbic System. To determine if subocrtical networks follow a different timeline, I analyzed the Limbic system (Figure 4). Unlike the Prefrontal Cortex, the Limbic network showed a distinct topological profile characterized by a specific reogranization during adolescence.

Global Efficiency followed a N shape trajectory, peaking in Infancy but dropping significantly in Adolescence ($p_{adj} = 0.003$ vs Infancy) before recovering in Adulthood. This suggests a transient reduction in network integration during puberty. In parallel, modularity in the limbic system displayed an inverse trajectory. Similar to the cortex, modularity dropped in infancy, representing integration. However, limbic modularity spiked significantly during adolescence ($p_{adj} < 0.001$ vs Infancy) before settling in Adulthood. This suggests a unique period of segregation in the limbic system during puberty.

Regarding control properties, the limbic system showed again a multi-phasic trajectory. Average controllability increased between Prenatal and Infancy ($p_{adj} < 0.001$), dropped at Adolescence ($p_{adj} < 0.001$ vs Infancy) and increased again in Adulthood ($p_{adj} < 0.001$ vs Adolescence). As in the Prefrontal Cortex, modal controllability replicated the average controllability trajectory, suggesting that the capacity for plasticity and specialization fluctuates in tandem in gene networks.

Discussion

The development of the human brain is defined not merely by growth of the organ, but by a profound architectural reorganization (1). While neuroimaging has long established that functional networks shift from a local anatomical scaffold to a distributed functional hierarchy (2, 3), the molecular mechanisms driving this topological metamorphosis have remained unknown. In this study, I integrated transcriptomics with network neuroscience to demonstrate that this reorganization is encoded in the co-expression patterns of the genome itself (Figure 2).

To do so, I first used Graph Theory to map the changing topography of gene co-expression. This analysis focused on two principles: integration, measured by Global Efficiency (the speed of information transfer across the whole network), and segregation, measured by Modularity (the partitioning of the network into autonomous communities). Rather than a monotonic maturation, the trajectory I observed in the Prefrontal Cortex reveals is non-linear (Figure 3). The network goes into a state of hyper-integration during

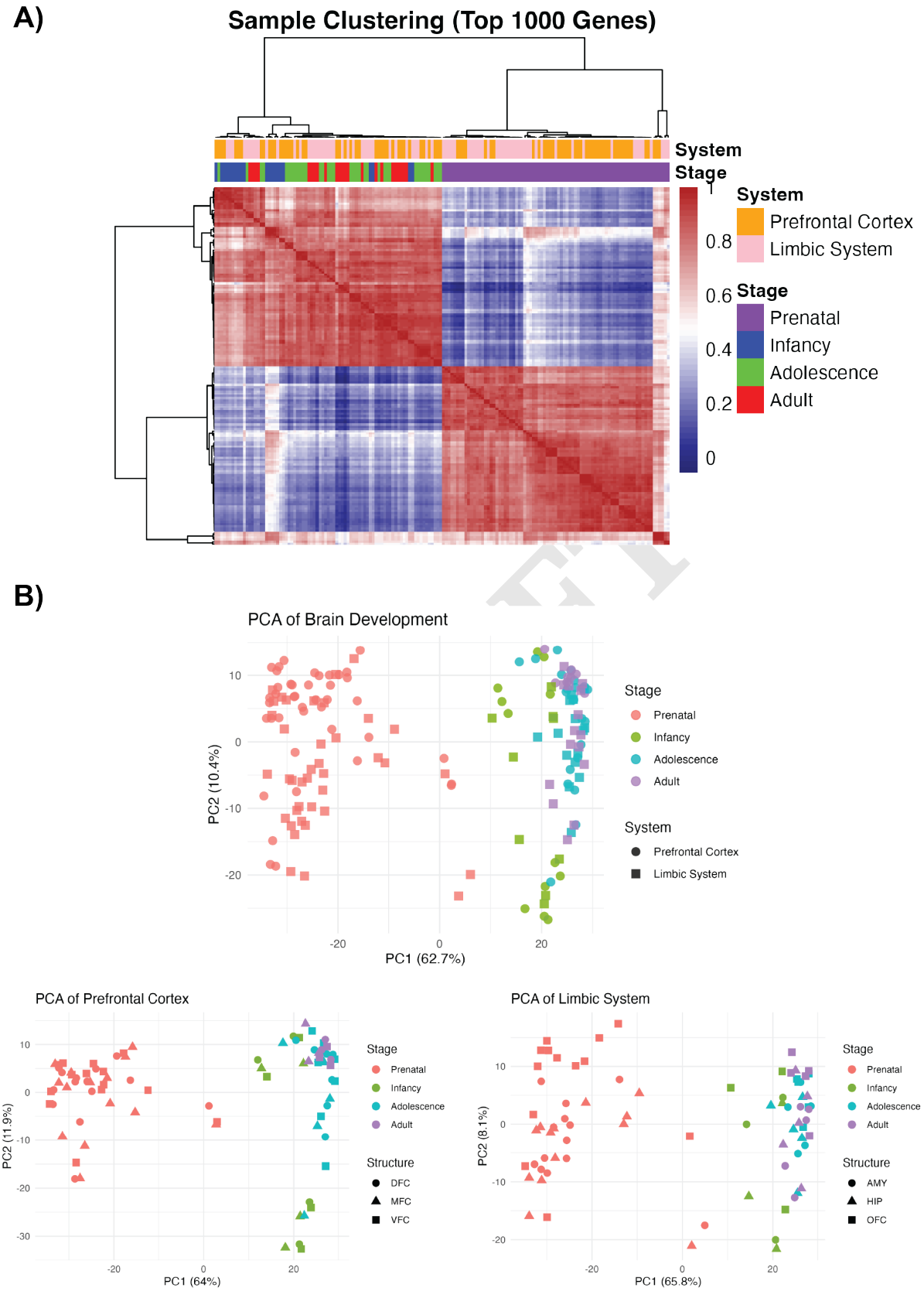

Fig. 1. Clustering Analyses (A) Heatmap of sample-to-sample correlation. (B) Principal component analyses of all the sample (top), prefrontal cortex (bottom left), and limbic system (bottom right).

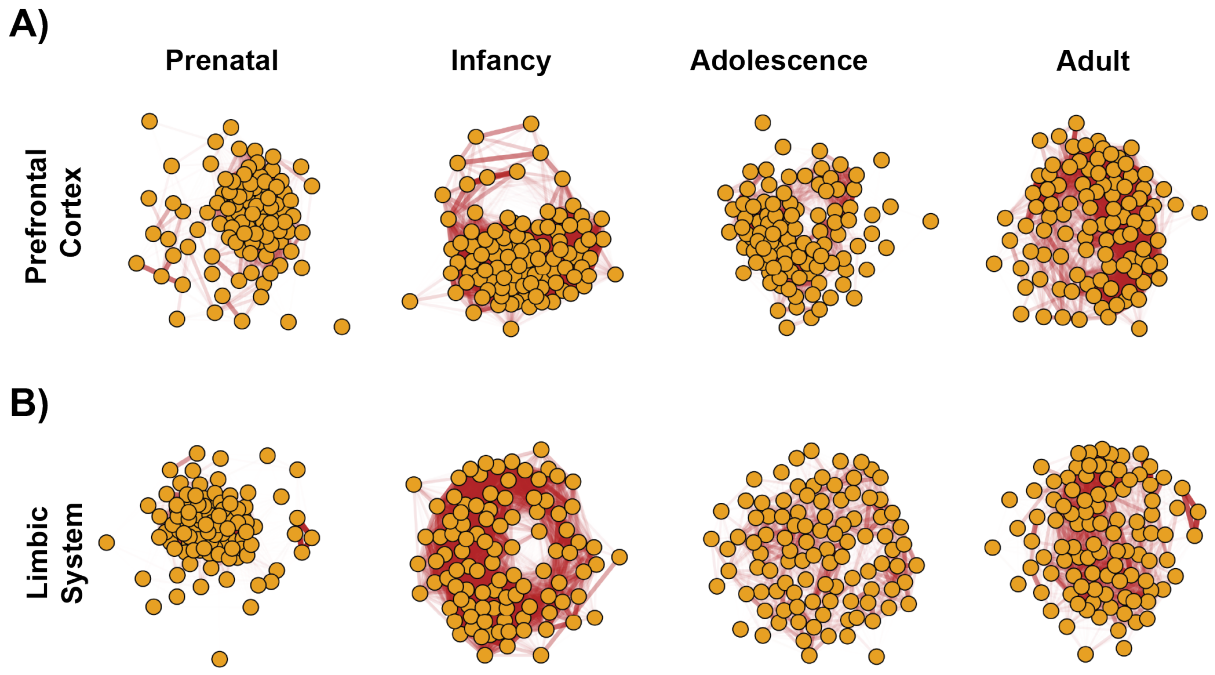

Fig. 2. Developmental Networks Visualization of gene co-expression networks (nodes = genes, edges = correlations) (A) for the prefrontal cortex (B) and limbic system across four developmental stages.

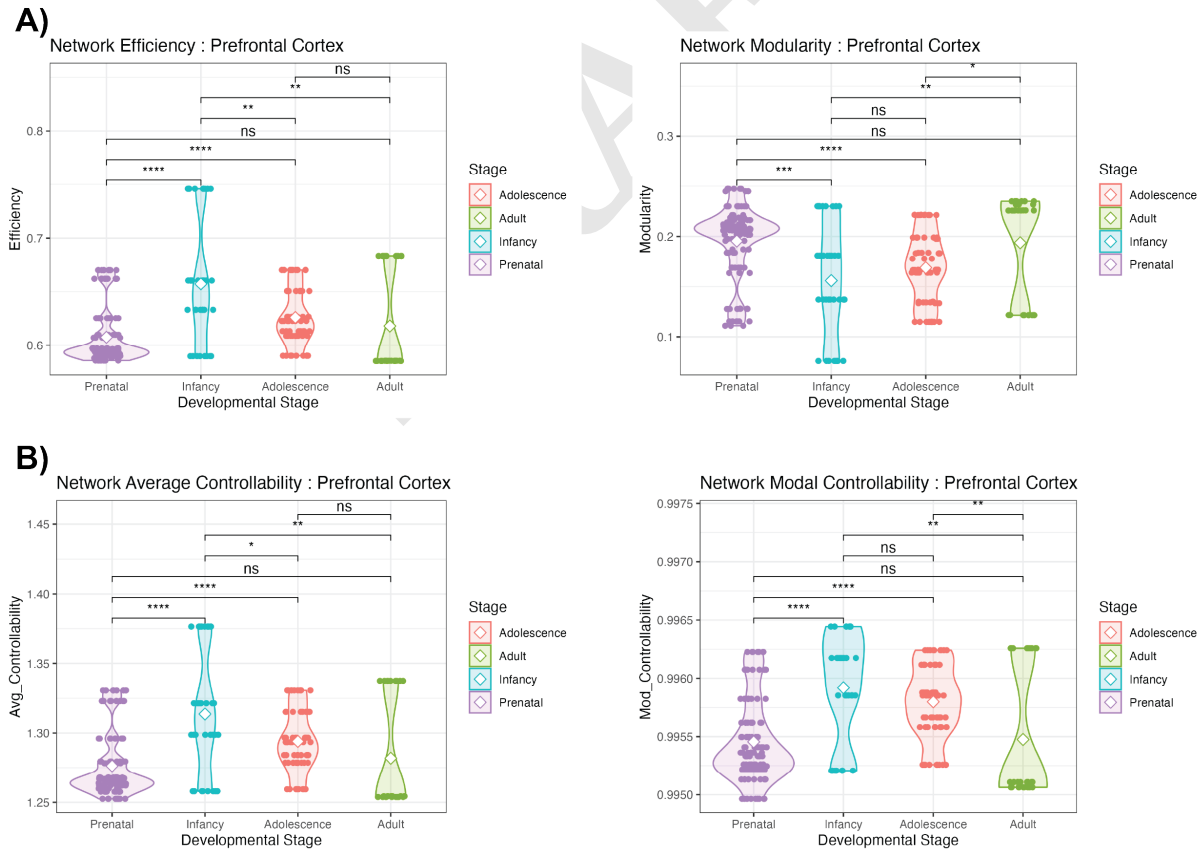

Fig. 3. Topological and network controllability analyses of the prefrontal cortex across development Violin plots showing the developmental trajectories of (A) global efficiency, (B) modularity, (C) average controllability, (D) and modal controllability. Statistics derived from one-way ANOVA, post-hoc Bonferroni corrected.

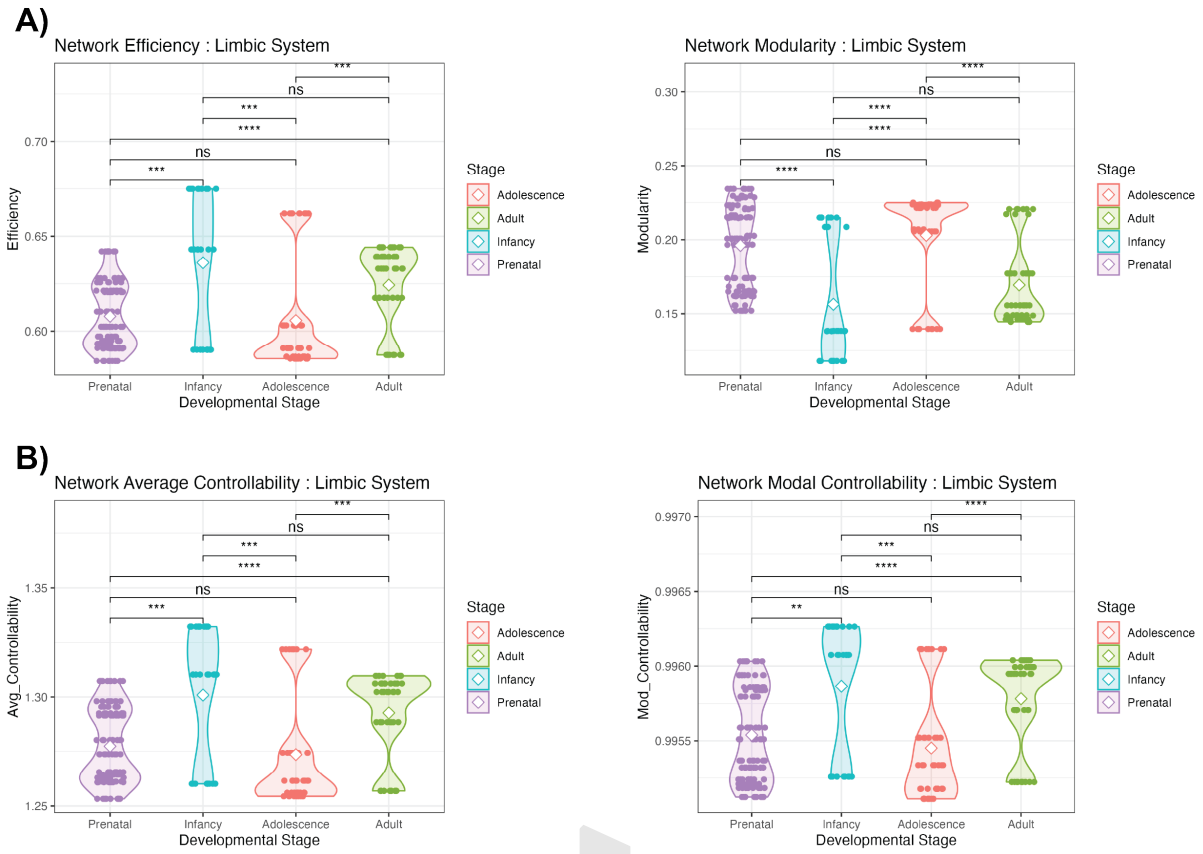

Fig. 4. Topological and network controllability analyses of the limbic system across development Violin plots showing the developmental trajectories of (A) global efficiency, (B) modularity, (C) average controllability, (D) and modal controllability. Statistics derived from one-way ANOVA, post-hoc Bonferroni corrected.

infancy before reorganizing into a segregated architecture in adulthood. This suggests that the infant connectome is temporarily wired for maximum connectivity, prioritizing the rapid assimilation of information over the specialized processing that characterizes the mature brain.

To interpret the functional consequences of this architecture, I applied Network Control Theory (NCT), a framework that quantifies how brain dynamics arise from the structural connectome (12, 14). By operationalizing controllability as an energy-based measurement, NCT assesses the ease of switching between brain states(12): Average Controllability measures the capacity to drive the brain toward nearby, easy-to-reach states, while Modal Controllability measures the capacity to steer the brain toward distant, difficult states. The hyper-integrated topology I observed in infancy coincided with a peak in Average Controllability. While previous work has established that network controllability develops rapidly during the perinatal period to support emerging cognitive demands (11), by amplifying the scope of analysis to include adolescence and adulthood, I show that this trajectory is not continuous. Instead, the increase in plasticity is unique to infancy. Biologically, this corresponds to the period of increased synaptogenesis and learning maximization. A network with low modularity and high Average Controllability is energetically inexpensive to navigate, allowing diverse inputs to easily drive global brain states (12). This suggests that the infant transcriptomic network is optimized for broad exploration before pruning into specialized, segregated modules observed in adulthood.

To determine if subcortical networks follow a different developmental timeline than the cortex, I analyzed the Limbic System (Figure 4). Unlike the Prefrontal Cortex, the Limbic network showed a distinct topological profile characterized by a specific reorganization during adolescence. Global Efficiency, Modularity, and Average and Modal Controllability all exhibited a significant multi-phasic trajectory, marked by a transient period of decreased integration and reduced control capacity during adolescence before stabilizing in adulthood. This suggests that the limbic system undergoes a unique period of topological isolation and constrained plasticity during puberty.

These findings should be interpreted in light of several limitations. First, the binning of development into four broad stages may smooth out finer-grained temporal shifts; a continuous analysis using sliding windows could provide a higher-resolution timeline of exactly when these topological phase transitions occur. Second, the grouping of distinct anatomical subregions into broad functional systems was necessary to ensure sufficient sample sizes for robust network construction. However, this aggregation masks potential heterogeneity; studying subregions individually would be beneficial to understand how these topological changes vary spatially with greater anatomical precision. Third, computational constraints limited this analysis to the top 500 most variable genes. Future analyses incorporating the

entire transcriptomic matrix would be useful to capture the full complexity of the gene regulatory network, including interactions among lower-variance genes that may still be topologically relevant. Finally, as this is a bulk tissue analysis, the observed network changes reflect an average across all cell types present in the sample. Consequently, the contributions of rare but developmentally important cell populations may be diluted by the dominant signal from abundant cell types(15). Future studies using single-cell transcriptomics are necessary to disentangle the cell-type-specific changes of these topological shifts.

Conclusion

This study establishes a transcriptomic basis for the macroscopic reorganization of the human brain. I demonstrated that the brain dynamics globally shared nor linear but undergo system- and age-specific transitions. The Prefrontal Cortex is wired for maximum integration and plasticity in infancy to facilitate rapid learning, while the Limbic System undergoes a unique period of topological isolation during adolescence. This framework could help understand how the brain balances the competing demands of plasticity, efficiency, and specialization across the lifespan, offering new insight into the molecular timing of neurodevelopmental vulnerability.

Materials and Methods

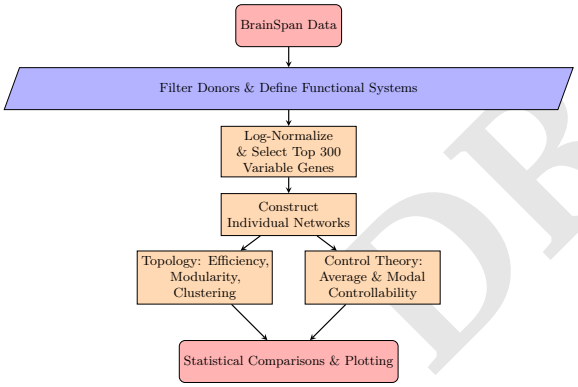

Fig. 5. Schematic of the data analysis workflow.

Data Acquisition and Pre-processing. Normalized gene expression data (RPKM) and associated metadata were obtained from the BrainSpan Atlas of the Developing Human Brain (10). The dataset comprises RNA-sequencing samples from donors ranging in age from 8 post-conception weeks (pcw) to 40 years. Donors were filtered to include only those with tissue samples available for the functional systems of interest. Developmental stages were based on established structural and functional milestones (13): Prenatal (8 - 37 post-conceptual weeks [pcw]), Infancy (4 months - 4 years), Youth/Adolescence (8 - 21 years), Adulthood (23+ years).

Samples were assigned to one of two functional systems: Prefrontal Cortex (comprising Dorsolateral Prefrontal [DFC], Ventrolateral Prefrontal [VFC], and Medial Prefrontal [MFC] cortices) and the Limbic System (comprising Orbital Frontal Cortex [OFC], Amygdala [AMY], and Hippocampus [HIP]).Gene expression counts were log-transformed ($\log_2(\text{RPKM} + 1)$) to stabilize variance.

Construction of Individual Gene Co-Expression Networks. To identify biologically relevant signal, feature selection was performed by identifying the top $N = 300$ most variable genes within each functional system across all donors. A gene-gene adjacency matrix was constructed by calculating the Pearson correlation coefficient between expression profiles.

To define the network topology while minimizing noise, I applied a soft-thresholding power of $\beta = 3$ where $A_{ij} = corr(i,j)^{\beta}$, suppressing weak correlations while preserving a weighted network. Self-loops were removed (diagonal set to zero), and correlations were absolutize ($abs(corr)$) to focus on co-regulation.

Network Topology metrics. Graph-theoretical metrics were calculated using the igraph package in R (16).

- **Global Efficiency:** Computed as the average inverse shortest path length.

$$E_{glob} = \frac{1}{N(N-1)} \sum \frac{1}{d_{ij}}$$

where N is the number of nodes and dij is the shortest path length between node i and node j.

- **Modularity:** Calculated using the Louvain community detection algorithm to quantify the extent to which the network is partitioned into dense functional modules.

$$Modularity = \frac{1}{2m} \sum_{i,j} \left[A_{ij} - \frac{k_i k_j}{2m} \right] \delta(c_i, c_j)$$

where m is the total weight of all edges in the network, A_{ij} is the weight of the edge between node i and node j, k_i is the degree of node i, c_i is the community assignment of node i, and $\delta(c_i, c_j)$ is the Kronecker delta function (1 if $c_i = c_j$, 0 otherwise) (17, 18).

Network Controllability Analysis. I applied Network Control Theory to model the energy landscape of the transcriptomic networks, following the framework established by Gu et al. (2015) (12).

Two control metrics were calculated for each network using the nctpy Python package:

- **Average Controllability:** Defined as the trace of the controllability Gramian ($\text{Tr}(W_c)$). This metric quantifies the system's capacity to move into easy, nearby states with low energy cost and serves as a proxy for network plasticity.

$$Tr(W_k) = \sum_{i=0}^{\infty} Tr(A^i B_k B_k^T (A^T)^i)$$

- **Modal Controllability:** Calculated based on the eigenvector alignment with the network's modes. This metric quantifies the capacity to drive the system into difficult, distant states (corresponding to small eigenvalues) and serves as a proxy for network specialization

$$\phi_i = \sum_{j=1}^{N} (1 - \lambda_j^2) v_{ij}^2$$

where v_{ij} is the i-th element of the j-th eigenvector of A, and λ_j represents the decay rate.

Visualization of Consensus Networks. For visualization purposes (Figure 2), Consensus Networks were generated for each developmental stage by pooling all tissue samples from all donors within that stage. To improve visual clarity, only the top 100 most variable genes were used to create the networks.

Statistical Analysis. Statistical comparisons between developmental stages were performed using one-way ANOVA on the individual donor metrics. Post-hoc pairwise comparisons were conducted using two-sample t-tests with Bonferroni correction for multiple comparisons. Statistical significance was defined as $p_{adj} < 0.05$. All analyses were performed in R using the stats and ggpubr packages.

Code Availability. All analysis code is available at: https://github.com/guillemchillon/Chillon_2025_NetworkAnalysis.

1. J Stiles, TL Jernigan, The Basics of Brain Development. *Neuropsychol. Rev.* **20**, 327–348 (2010).
2. DA Fair, et al., Functional Brain Networks Develop from a "Local to Distributed" Organization. *PLoS Comput. Biol.* **5**, e1000381 (2009).
3. DS Grayson, DA Fair, Development of large-scale functional networks from birth to adulthood: A guide to the neuroimaging literature. *NeuroImage* **160**, 15–31 (2017).
4. MP Van Den Heuvel, O Sporns, Network hubs in the human brain. *Trends Cogn. Sci.* **17**, 683–696 (2013).
5. DA Amado, et al., AAV-based delivery of RNAi targeting ataxin-2 improves survival and pathology in TDP-43 mice. *Nat. Commun.* **16**, 5334 (2025).
6. EM Carrell, MS Keiser, AB Robbins, BL Davidson, Combined overexpression of ATXN1L and mutant ATXN1 knockdown by AAV rescue motor phenotypes and gene signatures in SCA1 mice. *Mol. Ther. - Methods & Clin. Dev.* **25**, 333–343 (2022).
7. AA Van Berkel, et al., Dysregulation of Synaptic and Developmental Transcriptomic/Proteomic Profiles upon Depletion of MUNC18-1. *eneuro* **9**, ENEURO.0186–22.2022 (2022).
8. R Yang, et al., Upregulation of SYNGAP1 expression in mice and human neurons by redirecting alternative splicing. *Neuron* **111**, 1637–1650.e5 (2023).
9. J Richiardi, et al., Correlated gene expression supports synchronous activity in brain networks. *Science* **348**, 1241–1244 (2015).
10. M Li, et al., Integrative functional genomic analysis of human brain development and neuropsychiatric risks. *Science* **362**, eaat7615 (2018).
11. H Sun, et al., Network controllability of structural connectomes in the neonatal brain. *Nat. Commun.* **14**, 5820 (2023).
12. S Gu, et al., Controllability of structural brain networks. *Nat. Commun.* **6**, 8414 (2015).
13. S Oldham, A Fornito, The development of brain network hubs. *Dev. Cogn. Neurosci.* **36**, 100607 (2019).
14. YY Liu, JJ Slotine, AL Barabási, Controllability of complex networks. *Nature* **473**, 167–173 (2011).
15. GS Gulati, JP D'Silva, Y Liu, L Wang, AM Newman, Profiling cell identity and tissue architecture with single-cell and spatial transcriptomics. *Nat. Rev. Mol. Cell Biol.* **26**, 11–31 (2025).
16. G Csardi, T Nepusz, The igraph software package for complex network research. *arXiv* (year?).
17. MEJ Newman, Analysis of weighted networks. *Phys. Rev. E* **70**, 056131 (2004).
18. VD Blondel, JL Guillaume, R Lambiotte, E Lefebvre, Fast unfolding of communities in large networks. *J. Stat. Mech. Theory Exp.* **2008**, P10008 (2008).